

CONF-8106191--2

DE83 009671

ELECTRON-ELECTRON CORRELATION IN HIGHLY CHARGED ATOMS

W.R. Johnson and K.T. Cheng

Department of Physics
University of Notre Dame
Notre Dame, Indiana 46556
and
Argonne National Laboratory
Argonne, Illinois 60439

ABSTRACT

The relativistic random-phase approximation (RRPA) is introduced to account for electron-electron correlation in atoms and ions of high nuclear charge where non-relativistic many-body methods are inadequate. To provide a basis for this study of the RRPA, the Dirac-Fock (DF) theory is reviewed. Applications of the DF equations to determine inner-electron binding energies in heavy atoms are given illustrating the influence of relativistic effects in situations where correlations are unimportant. The RRPA equations are derived as natural generalizations of the DF equations. Examples of RRPA calculations of discrete excitations and of photoionization are given illustrating situations where both relativistic and correlation effects play important roles.

I. REVIEW OF THE DIRAC-FOCK THEORY

To set a framework for our study of correlation effects in highly charged atoms we briefly review the central field DF approach to atomic structure calculations. The Dirac-Fock theory is based on an approximate relativistic Hamiltonian¹

NOTICE
PORTIONS OF THIS REPORT ARE ILLEGIBLE.
It has been reproduced from the best available copy to permit the broadest possible availability.

DISTRIBUTION OF THIS REPORT IS UNLIMITED

JHR

MASTER

$$H_0 = \sum_{i=1}^N h_i + \sum_{i>j} \frac{e^2}{r_{ij}} \quad (1.1)$$

where $h = \vec{\alpha} \cdot \vec{p} + \beta m - e^2 Z/r$ is the usual one-electron Dirac Hamiltonian. Although the application of H_0 to atomic structure problems has been criticized,³⁻⁵ its use in connection with DF calculations has been recently justified from the point of view of quantum electrodynamics.⁶ A DF wave function is constructed as a Slater determinant of single-electron Dirac orbitals $u_i(\vec{r})$ in parallel with the usual non-relativistic Hartree-Fock (HF) procedure. These orbitals $u_i(\vec{r})$ are assumed to be orthonormal positive energy solutions to a central field Dirac equation. The expectation value of the Hamiltonian H_0 in Eq. (1.1) is then expressed as a functional of the orbitals $u_i(\vec{r})$ and the variational principle is applied to this functional to obtain the DF equations for the orbitals u_i :

$$(h+V)u_i = \epsilon_i u_i \quad i=1, \dots, N \quad (1.2)$$

The quantity V is a self-consistent DF potential

$$V u = \sum_{i=1}^N e^2 \int \frac{d^3 r'}{|\vec{r}-\vec{r}'|} [(u_i^\dagger u_i)' u - (u_i^\dagger u)' u_i] \quad (1.3)$$

The equations (1.2) and (1.3) are similar to the non-relativistic HF equations but there are two important differences; the single-electron Hamiltonian h is a Dirac Hamiltonian and the orbitals $u_i(\vec{r})$ are Dirac orbitals. The Dirac orbitals $u_i(\vec{r})$ may be separated into radial and spin-angle functions and Eqs. (1.2) and (1.3) reduced to coupled radial equations.⁷ Positive energy solutions to the resulting radial self-consistent field equations may then be obtained numerically.⁸

The DF eigenvalue ϵ_i has the physical significance of being the "frozen-orbital" approximation to the binding energy of an electron in state i .⁹ To get some notion of the importance of relativistic effects in situations where correlation is expected to be insignificant we compare the non-relativistic HF eigenvalues and the relativistic DF eigenvalues with experimentally measured K-shell binding energies.

In Figure 1 we plot experimental K-shell binding

energies determined by Bearden and Burr¹⁰ against Z . It is interesting to note that the non-relativistic Coulomb binding energy of a $1s$ electron ($Z^2 \text{ Ry}$) gives a good approximation to the data in Figure 1, but this agreement arises only because of an accidental cancellation between relativistic and screening effects.

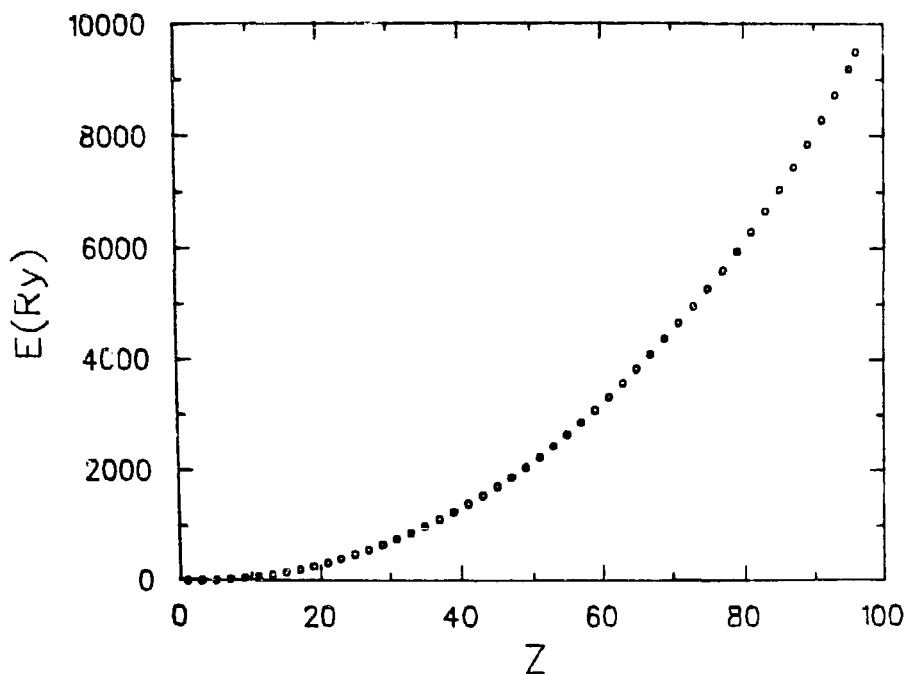


Fig. 1. Experimental K-shell binding energies as determined by Bearden and Burr, Ref. 10, are plotted against nuclear charge.

In Fig. 2 HF eigenvalues¹¹ and DF eigenvalues¹² are compared with the data from Figure 1. The error in the HF approximation varies from -3% at $Z=10$ to 12% at $Z=90$. The error at low Z is primarily due to the relaxation and correlation effects not included in the "frozen-orbital" HF approximation while the error at high Z is mainly due to relativity. To see that this is indeed the case we note that the DF approximation in Fig. 2 agrees with the HF approximation at low Z where electronic velocities are small and reduces the discrepancy between the HF approximation and measurement

from 12% to -1% at high Z. It is of interest to examine the extent to which the residual difference between the DF approximation and measurement shown in Fig. 2 can be accounted for without considering correlation effects.

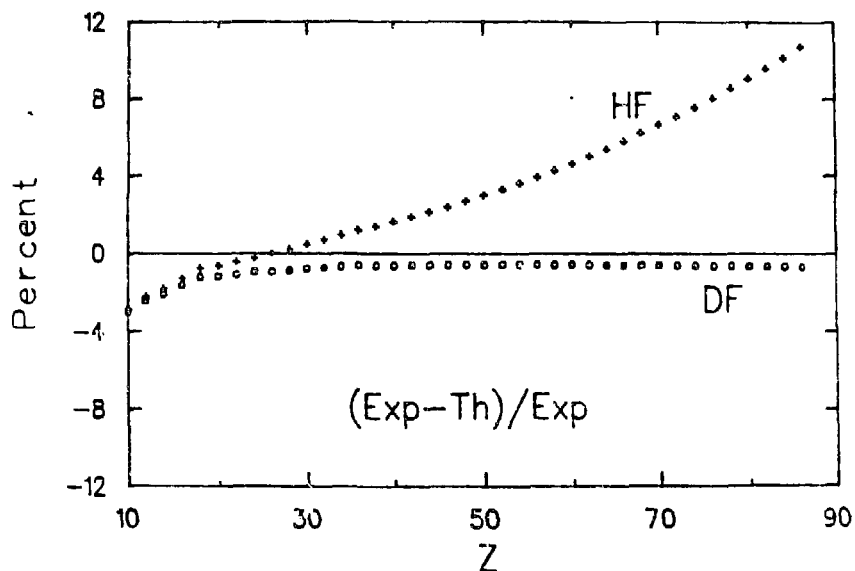


Fig. 2. Relative difference between frozen orbital calculations of K-shell binding energies and the measurements of Ref. 10. HF calculations are from Ref. 11 and DF calculations are from Ref. 12.

Before discussing this problem it should be mentioned that the DF calculations used in Fig. 2 include the effects of finite nuclear size on the atomic orbitals. These finite size effects are incorporated in the single-electron Hamiltonian h by replacing the Coulomb potential by a potential due to the nuclear charge density $\rho(\vec{r})$:

$$-\frac{e^2 Z}{r} \rightarrow e \int \frac{\rho(\vec{r}')}{|\vec{r} - \vec{r}'|} d^3 r' \quad (1.4)$$

The nuclear charge density is taken to be a Fermi-distribution with parameters determined from electron-nucleus scattering measurements.¹³ Finite nuclear size corrections to K-binding energies grow roughly as Z^4 and reduce the theoretical K-binding energy in mercury ($Z=80$) by about 4 Ry.

Even within the DF framework the comparison of orbital eigenvalues with inner electron binding energies is incorrect since such a comparison ignores the relaxation of atomic orbitals when an inner electron is removed from the atom. To account for relaxation one must carry out separate DF calculations for the atom and ion and subtract the resulting total atomic and ionic energies. One then obtains

$$E(\text{atom}) - E(\text{ion}) = \epsilon_i - \Delta E_i \quad (1.5)$$

where ϵ_i is the DF eigenvalue of the atomic electron being removed and ΔE_i is a relaxation correction to the binding energy of that electron. For the K-shell of mercury the relaxation correction reduces the theoretical binding energy by about 7 Ry.

Table I. Binding Energies of Inner-Shell Electrons (eV) of Noble Gas Atoms.

Shell	Z	Frozen ^a	Relaxed ^b	Experiment
Argon	18			
K		3241.6	3209.2	3206.0 ^c
L _I		337.7	327.2	
L _{II}		262.1	250.5	247.3(3) ^d
L _{III}		259.8	248.3	245.2(3)
Krypton	36			
K		14413.6	14359.3	14325.6(8)
L _I		1961.4	1933.6	1921.2(6)
L _{II}		1765.4	1735.0	1727.2(5)
L _{III}		1711.1	1681.3	1674.9(5)
Xenon	54			
K		34756.3	34690.0	34561.4(11)
L _I		5509.4	5472.4	5453.8(4)
L _{II}		5161.5	5120.4	5103.7(4)
L _{III}		4835.6	4796.0	4782.2(4)

a) Ref. 12, b) Ref. 14, c) Ref. 15, d) Ref. 10

The effect of including relaxation on inner electrons is illustrated in Table I where we list frozen-orbital,¹² relaxed¹⁴ and experimental binding energies^{10,15} for the inner K- and L- shells of the noble gases argon, krypton, and xenon. For the K-shell of argon the 1% error in the frozen orbital

approximation is reduced to about 0.1% while in krypton the error is reduced from 0.6% to 0.2% and in xenon from 0.6% to 0.4%. The situation for L-shells is quite similar, inclusion of relaxation effects in inner-shell binding calculations improves the agreement between the DF approximation and experiment substantially.

From Table I we see that the residual difference between theory and experiment is a rapidly increasing function of nuclear charge. This residue is due in part to the omission of terms arising from transverse photon exchange in the Hamiltonian H_0 . Such terms lead to a frequency dependent modification^{1,16} of the Breit interaction, viz:

$$H_{\text{trans}} = -e^2 \left\{ \frac{\cos \omega R}{R} \vec{a}_1 \cdot \vec{a}_2 + \vec{a}_1 \cdot \vec{\nabla} \vec{a}_2 \cdot \vec{\nabla} \frac{\cos \omega R - 1}{\omega^2 R} \right\}, \quad (1.6)$$

where $R = |\vec{r}_1 - \vec{r}_2|$ and $\omega = \epsilon_1 - \epsilon_2$. Neglecting terms of order $(\omega R)^2 \sim a^2 Z^2$ the transverse interaction reduces to the Breit interaction¹.

$$H_{\text{Br}} = -\frac{e^2}{2R} (\vec{a}_1 \cdot \vec{a}_2 + \vec{a}_1 \cdot \vec{R} \vec{a}_2 \cdot \vec{R}). \quad (1.7)$$

The influence of the Breit interaction on the binding energies of K-, L-, and M-shell electrons in mercury is illustrated in Table II. In the second column we list the relaxed DF energies as determined by Huang et al.,¹⁷ and in the third column we list the Breit correction to these energies as obtained from a relaxed perturbation theory calculation. Comparison of the resulting DF + Breit energies with the experimental values shows that the Breit interaction accounts for a major part of the discrepancy between the relaxed DF eigenvalues and experiment.

Table II. Breit Interaction and QED Corrections to Inner Shell Binding Energies (au) for Mercury.

Shell	DF ^a	Breit	DF+Breit	QED	Exp ^b
K	3070.7	-11.15	3059.6	3053.9	3054.2(3)
L _I	548.1	-1.23	546.9	546.0	545.5(3)
L _{II}	524.5	-2.09	522.4	522.4	522.3(2)
L _{III}	453.0	-1.32	451.7	451.6	451.6(2)
M _I	131.9	-0.22	131.7	131.7	131.1(4)
M _{II}	121.4	-0.39	121.0	121.0	120.7(5)
M _{III}	105.3	-0.23	105.1	105.1	104.8(2)
M _{IV}	88.1	-0.17	88.0	88.0	87.8(1)
M _V	84.7	-0.11	84.6	84.6	84.5(1)

a) Ref. 17, b) Ref. 10

Electron self-energy and vacuum polarization corrections account for most of the remaining difference between DF calculations and experiment. For high Z atoms the electron self-energy has been studied numerically by Desiderio and Johnson¹⁸ for 1s electrons with Z in the range of 70-90 using the method outlined by Brown, Langer and Schaefer,¹⁹ and by Mohr^{20, 21} for 1s, 2s, and 2p electrons with Z < 137. The effects of finite nuclear size on the 1s Lamb shift have been considered by Cheng and Johnson.²² Vacuum polarization in heavy atoms has been studied by Wichmann and Kroll^{23, 24} and the finite nuclear size corrections to vacuum polarization have been worked out by Gyulassy²⁵.

In column 5 of Table II the influence of the electron self-energy and vacuum polarization corrections on the binding energies of the inner shells of mercury are shown.¹⁷ The resulting theoretical values are seen to agree with the experimental measurements to within one or two times the experimental errors. This comparison for mercury is typical of other heavy atoms and leads to a high degree of confidence in DF calculations for those applications in which correlation effects are expected to be insignificant.

By correlation we understand those effects arising

from the difference between the electron-electron Coulomb interaction and the approximate DF central potential. In the following paragraphs we describe the RRPA which is a natural extension of the DF theory accounting for many of the important effects of correlation, and we give applications to photoexcitation and photoionization problems where both relativistic and correlation effects are significant.

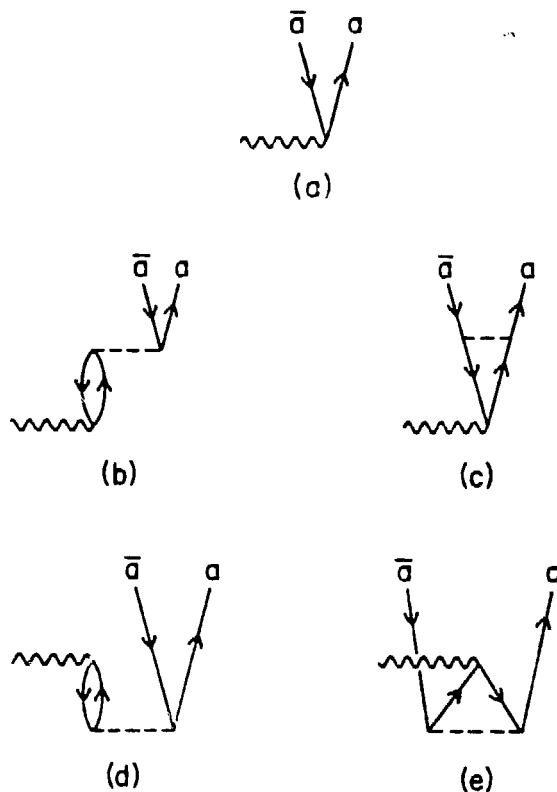


Fig. 3. Lowest order Feynman diagrams contributing to the RRPA amplitude.

————— Electron in a Dirac-Fock potential;

----- Coulomb part of the photon propagator;

~~~~~ External photon;  $a$  and  $\bar{a}$ , electron and hole labels, respectively.

## II. RELATIVISTIC RANDOM-PHASE APPROXIMATION

The governing equations of the RRPA may be developed from quantum electrodynamics using perturbation theory, or alternatively from time dependent Hartree-Fock (TDHF) theory. In the perturbation approach, the ground state is taken to be the Fermi-level of a closed-shell system with  $N$  electrons, and a diagrammatic method may be used to describe the excitation of the ground state caused by an external photon. The lowest order terms included in photoexcitation processes are illustrated in the Feynman diagrams of Fig. 3. The RRPA transition amplitude is obtained from these diagrams by iteration at the photon vertex.<sup>26</sup>

In Fig. 3, we consider only the Coulomb part of the electron-electron interaction and omit the transverse part which leads to the Breit interaction. We also omit radiative corrections which lead to the Lamb shift. Errors due to the omission of the Breit interaction and the Lamb shift are insignificant for many practical applications, and when corrections for these effects are required, they may be accounted for as perturbations.<sup>27</sup> Errors due to the omitted Coulomb terms in higher order diagrams, on the other hand, are more difficult to assess; nevertheless, experience with a large number of applications of the non-relativistic random-phase approximation with exchange (RPAE) shows that such calculations in general agree very well with experimental measurements.<sup>28</sup> In the past few years, there have been extensive applications of the RRPA to photoexcitation<sup>27, 29-36</sup> and photoionization.<sup>37-47</sup> A brief account of the RRPA theory will be given in the next few paragraphs, followed by examples of these calculations.

As mentioned previously, the RRPA equations can be obtained by linearizing the TDHF equations<sup>48</sup> describing the response of an atom to a time dependent external field  $v(t)$ . The Hamiltonian of the system is given by:

$$H = H_0 + \sum_{i=1}^N v_i(t) \quad , \quad (2.1)$$

where  $H_0$  is the approximate relativistic Hamiltonian given in<sup>0</sup> Eq. (1.1). Starting from the time dependent variational principle<sup>49</sup>

$$\langle \delta\Psi | H - i \frac{\partial}{\partial t} | \Psi \rangle = 0 \quad , \quad (2.2)$$

we seek a stationary solution to the above equation with the trial wavefunction:

$$\Psi(\vec{r}_1, \vec{r}_2, \dots, \vec{r}_N, t) = \frac{1}{\sqrt{N!}} \begin{vmatrix} \phi_1(\vec{r}_1, t) & \dots & \phi_1(\vec{r}_N, t) \\ \vdots & & \vdots \\ \phi_N(\vec{r}_1, t) & \dots & \phi_N(\vec{r}_N, t) \end{vmatrix} \quad (2.3)$$

In the absence of the time dependent external field, the single electron Dirac wave functions are given by  $\phi(\vec{r}, t) = u(\vec{r})e^{-i\epsilon t}$ , and the variational calculation leads to the usual Dirac-Fock (DF) equations for the atomic ground state given in Eqs. (1.2) and (1.3). Application of a time dependent external field,  $v(t) = v_+ e^{-i\omega t} + v_- e^{i\omega t}$  induces a time dependent perturbation to the orbitals:

$$u(\vec{r}) \rightarrow u(\vec{r}) + w_+(\vec{r})e^{-i\omega t} + w_-(\vec{r})e^{i\omega t} + \dots \quad (2.4)$$

Neglecting higher order terms, the RRPA equations for the first order perturbed orbitals,  $w_{i\pm}$ , can be obtained from the linearized TDHF equations as:

$$[h + V - (\epsilon_{i\pm} + \omega)] w_{i\pm} = -V_{\pm}^{(1)} u_i, \quad i = 1, 2, \dots, N \quad , \quad (2.5)$$

where the first order perturbed potential  $V_{\pm}^{(1)}$  is given by:

$$V_{\pm}^{(1)} u_i = \sum_{j=1}^N \int \frac{d^3 r'}{|\vec{r} - \vec{r}'|} [(u_j^{\dagger} w_{j\pm})' u_i - (u_j^{\dagger} u_i)' w_{j\pm} + (w_{j\pm}^{\dagger} u_j)' u_i - (w_{j\pm}^{\dagger} u_i)' u_j] \quad (2.6)$$

If we leave out the driving term  $-V_{\pm}^{(1)} u_i$ , Eq. (2.5) reduces to the excited state DF equation for  $w_{i+}$ , with excitation energy  $\omega$  (there is no non-trivial physical solution to  $w_{i-}$  in the DF approximation for  $\omega \ll 2mc^2$ ). Correlation effects are included in the RRPA through the

perturbed potential  $V^{(1)}$  which induces couplings between excitation channels  $u_i \leftrightarrow w_{i\pm}$ . The eigenvalues  $\omega$  of Eq. (2.5) provide an approximation to the excitation spectrum of the atom, including a discrete range and a continuum. The positive frequency components of the eigenfunctions,  $w_{i+}$ , describe atomic excited states including final state correlations illustrated in Fig. 3(b,c), while  $w_{i-}$  describes ground state correlations illustrated in Fig. 3(d,e). More detailed discussions of the RRPA equations and their physical implications can be found in Refs. 40 and 50.

In radiative processes, the electron-photon interaction in the Coulomb gauge is given by  $v_+ = e\vec{a}\cdot\vec{A}$  and  $v_- = v_+$ . The transition amplitude from the ground state to an excited state is then given by:

$$T = \sum_{i=1}^N e \int d^3r [w_{i+}^{\dagger} \vec{a}\cdot\vec{A} u_i + u_i^{\dagger} \vec{a}\cdot\vec{A} w_{i-}] \quad (2.7)$$

An important property of the RRPA transition amplitude is that it is gauge invariant. The oscillator strengths calculated in the length gauge are the same as those calculated in the velocity gauge in contrast to other approximate many-body methods (such as DF theory applied to excited states) which give gauge dependent transition amplitudes. In practical applications, we usually truncate the RRPA equations to simplify numerical calculations, with the result that the transition amplitudes are no longer gauge invariant. The degree of gauge dependence can then be used as a measure of the truncation error.

The RRPA has been applied to treat discrete excitations in highly stripped ions where both relativity and correlation are important. Allowed and forbidden transitions for ions in the He,<sup>27</sup> Be,<sup>29-31</sup> Mg,<sup>32</sup> Zn<sup>34,35</sup> and Ne<sup>36</sup> sequences have been studied. We present selected examples here to illustrate the utility of the RRPA technique. A more detailed summary of these results is given in Ref. 51.

In the Be sequence, the electric dipole interaction induces four interaction channels:  $1s \rightarrow np_{1/2}$ ,  $np_{3/2}$  and  $2s \rightarrow np_{1/2}$ ,  $np_{3/2}$  (actually, there are eight coupled channels in RRPA calculations if we count positive and negative frequency channels separately). For the transition of the  $(2s^2)^1S$  ground state to the  $(2s2p)^1P^0$  excited state, we first omit contributions from  $1s$  channels and obtain truncated RRPA

values. As we can see from Table III, the agreement between length and velocity form oscillator strengths is poor for these "frozen-core" calculations. The full RRPA calculation including all excitation channels retains gauge invariance of the transition matrix elements, as reflected in the perfect agreement between length and velocity form results.

Table III. Oscillator Strengths of the Resonance Transition  $(2s^2)^1S-(2s2p)^1P^0$  for Be-like Ions.

|                   |          | Truncated RRPA <sup>a</sup> | Full RRPA <sup>a</sup> | MCDF <sup>b</sup> |
|-------------------|----------|-----------------------------|------------------------|-------------------|
| Ar <sup>14+</sup> | length   | 0.199                       | 0.198                  | 0.208             |
|                   | velocity | 0.228                       | 0.198                  | 0.173             |
| Mo <sup>38+</sup> | length   | 0.140                       | 0.140                  | 0.140             |
|                   | velocity | 0.151                       | 0.140                  | 0.134             |

a) Lin and Johnson, Ref. 32

b) Cheng and Johnson, Ref. 52

We include also in Table III the multiconfiguration Dirac-Fock (MCDF) results of Cheng and Johnson<sup>52</sup> for comparison purposes. As one can see, the length form results in all three calculations are in agreement with each other, while the velocity form results are quite sensitive to approximations involved in the calculations. This suggests that the length gauge may be preferred in transition calculations where gauge invariance is violated.

In Table IV, we present some results of a truncated RRPA calculations for Mg-like ions in which only excitations of the  $3s^2$  valence electrons are included and excitations of the core electrons are omitted. In spite of this approximation, the excitation energies of the resonance transition,  $(3s^2)^1S-(3s3p)^1P^0$ , are in good agreement with experiment. Furthermore, length and velocity form oscillator strengths agree to within one

Table IV. Excitation Energies  $\omega$  (in atomic units) and Length Form Oscillator Strengths  $f_L$  of the Resonance Transition  $(3s^2)1S-(3s3p)1P^o$ , for Mg-like Ions.

|          |                   | Ar <sup>6+</sup>    | Fe <sup>14+</sup>  | Mo <sup>30+</sup> |
|----------|-------------------|---------------------|--------------------|-------------------|
| $\omega$ | RRPA <sup>a</sup> | 0.7798              | 1.605              | 3.93              |
|          | MCDF <sup>b</sup> | 0.7928              | 1.628              | 3.97              |
|          | Experiment        | 0.7779 <sup>c</sup> | 1.604 <sup>d</sup> | 3.89 <sup>e</sup> |
| $f_L$    | RRPA <sup>a</sup> | 1.27                | 0.83               | 0.55              |
|          | MCDF <sup>b</sup> | 1.25                | 0.82               | 0.54              |

a) Shorer, Lin and Johnson, Ref. 33

b) Cheng and Johnson, Ref. 53

c) Mocre, Ref. 54

d) Cowan and Widing, Ref. 55

e) Hinnov, Ref. 56

or two percent, and are in good agreement with corresponding MCDF length form results of Cheng and Johnson.<sup>53</sup> The success of the frozen-core approximation in this case can be attributed to a tight Ne-like core. By contrast, a similar two-channel frozen-core calculation for the resonance transition,  $(4s^2)1S-(4s4p)1P^o$ , in Zn-like ions<sup>54</sup> no longer includes dominant correlation effects, as the  $3d^{10}$  core is easily polarized, resulting in 10-20% changes in the oscillator strengths when  $3d$  excitation channels are included in the calculation.<sup>55</sup>

The RRPA has been applied to studies of low energy atomic photoionization of rare gas atoms. Subshell cross sections as well as angular distribution and spin polarization of photoelectrons are calculated, and results are in good agreement with experiment. A few examples of these studies are presented here, with emphasis on the interplay between correlation and relativity in photoionization processes. Only length form RRPA results are given, as they agree with velocity form results to within a few percent in all these

calculations.

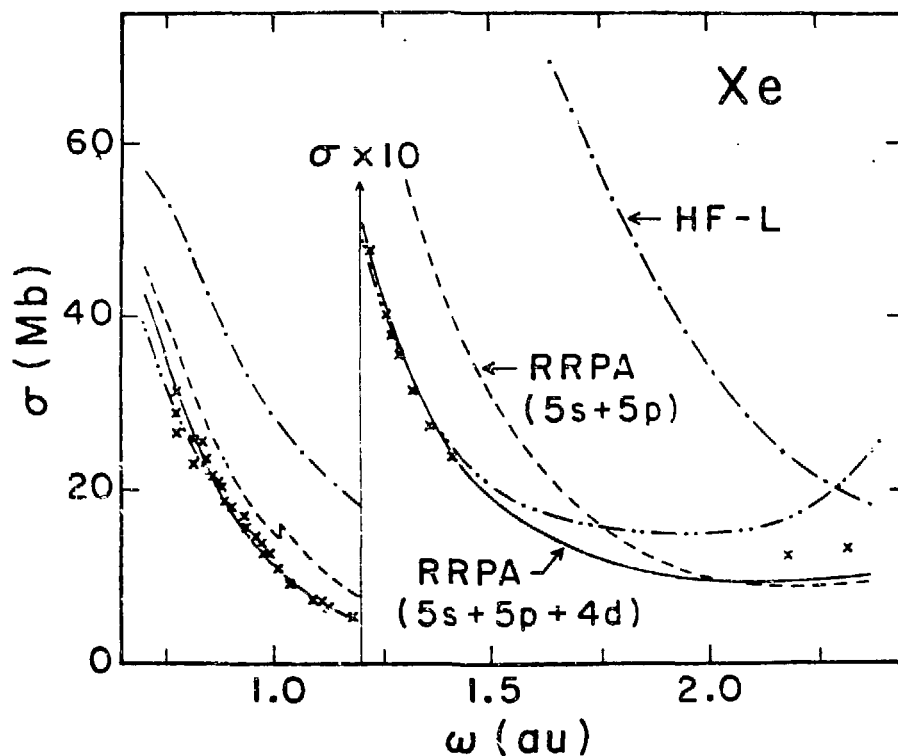


Fig. 4. Photoionization cross sections for xenon as functions of photon energy  $\omega$ . Experiment: — · — · — West and Morton, Ref. 57; X Samson, Ref. 58. Theory: — and — — — RRPA, three- and two-shell correlation results, respectively, Ref. 41; — · — Kennedy and Manson, Ref. 59.

#### i) Total Cross Sections

In Fig. 4, we show total photoionization cross sections for xenon atoms. One general observation that can be made is that correlation effects as measured by the difference between HF<sup>59</sup> and RRPA<sup>41</sup> results are sizeable. Moreover, the inclusion of excitation channels of the 4d shell in the RRPA calculation substantially improves the agreement between theory and experiment, reflecting the importance of core

polarization effects in xenon. It should be mentioned here that no relativistic effects show up in total cross sections and that RRPA results are generally in close agreement with nonrelativistic RPAE calculations<sup>28</sup> for rare gas atoms.

### ii) Partial Cross Section Branching Ratios

Non-relativistically, there is no distinction between subshells of the same fine structure, so the partial cross section branching ratio for two such subshells will be the "statistical ratio" given by their relative occupations. Experimentally, it has been known for some time that the branching ratios of outer  $np$  cross sections for rare gases depart from the statistical ratio of 2.<sup>60</sup> In Fig. 5, the RRPA branching ratios  $\sigma(5^2P_{3/2}) : \sigma(5^2P_{1/2})$  in xenon are compared with measurements<sup>60, 61</sup> and with DF<sup>62</sup> and Dirac-Slater (DS) results.<sup>61</sup>

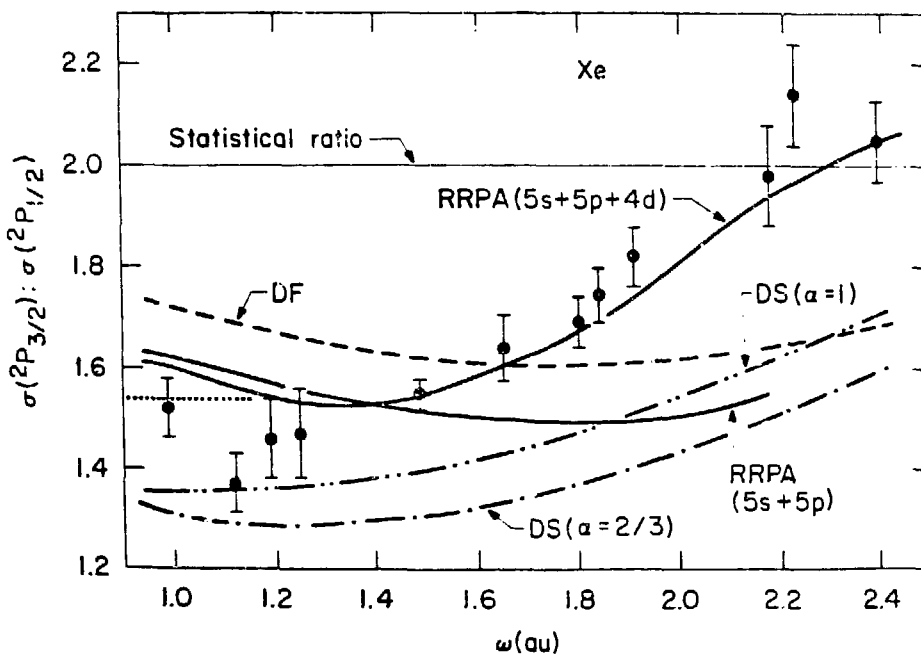


Fig. 5. The  $2P_{3/2} : 2P_{1/2}$  branching ratios for xenon as functions of photon energy  $\omega$ . Experiment: ..... Samson et al., Ref. 60;  $\frac{1}{2}$  Wuilleumier et al., Ref. 61. Theory ——— RRPA, Ref. 41; - - - - Ong and Manson, Ref. 62; - · - · - and · · · · · Wuilleumier et al., Ref. 61.

The three-shell (5s+5p+4d) RRPA calculation is seen to represent experimental values better than the uncorrelated calculation. Similar RRPA calculations have been reported for the  $\sigma(4^2D_{5/2}) : \sigma(4^2D_{3/2})$  branching ratio in xenon.<sup>39</sup> Because of the sensitivity of branching ratios to both correlation and relativity, such measurements provide interesting tests of relativistic many-body theories.

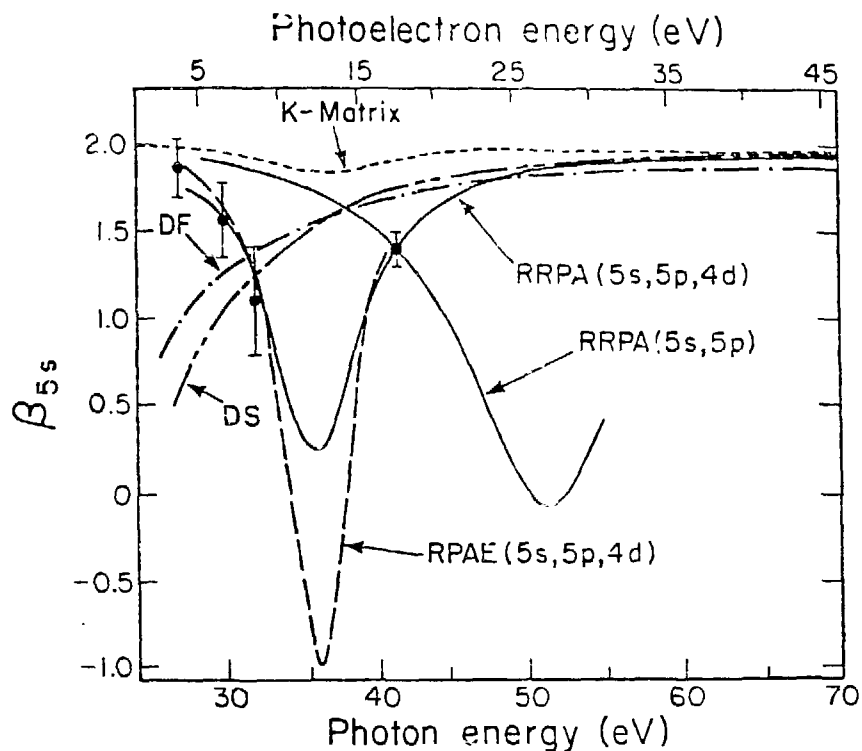


Fig. 6. The asymmetry parameters  $\beta$  for the 5s shell of xenon as functions of photon energy  $\omega$ . Experiment:  $\square$  Dehmer and Dill, Ref. 63;  $\circ$  White et al., Ref. 64. Theory: ——— RRPA, Refs. 38, 41; - - - Cherepkov, Ref. 65; - - - - Huang and Starace, Ref. 66; — · — Ong and Manson, Ref. 67; — · — Walker and Waber, Ref. 68.

### iii) Angular Distributions

In the dipole approximation, the photoionization differential cross section is given by:

$$\frac{d\sigma}{d\Omega} = \frac{\sigma}{4\pi} \left[ 1 - \frac{1}{2}\beta P_2(\cos\theta) \right] \quad (2.8)$$

Here,  $\theta$  is the angle between the photon momentum  $\vec{k}$  and the electron momentum  $\vec{p}$ ,  $\sigma$  is the photoionization cross section and  $\beta$  is the angular distribution asymmetry parameter.

For the  $5s \rightarrow \epsilon p$  photoionization in xenon, nonrelativistic calculation shows that  $\beta = 2$ , independent of photon energy, whereas relativistically,  $\beta$  can depart from 2 because of the interference between  $5s \rightarrow \epsilon p_{1/2}$  and  $5s \rightarrow \epsilon p_{3/2}$  channels. Experimentally, deviations from the value of 2 for  $p_{5s}$  have been observed near the Cooper minimum of the  $5s$  partial cross section.

As shown in Fig. 6, successful explanations of these data again come from relativistic many-body calculations which account for dominant correlation effects - in this case, the RRPA three-shell ( $5s$ ,  $5p$ ,  $4d$ ) correlation calculations.

### iv) Spin Polarization

Even with unpolarized incident radiation, the photoelectron is in general polarized in the direction perpendicular to the reaction plane defined by the incident radiation and the outgoing electron. In the dipole approximation, the degree of polarization  $P_y(\vec{y} // \vec{k} \times \vec{p})$  is given by:<sup>69-71</sup>

$$P_y = \frac{\eta \sin\theta \cos\theta}{1 - \frac{1}{2}\beta P_2(\cos\theta)} \quad (2.9)$$

In Fig. 7, the measured spin polarization parameters  $\eta$  of the  $5p$  shell are given, along with various theoretical results. Once again, we find good agreement between experiment<sup>72</sup> and the RRPA three-shell calculation.<sup>42</sup> Similar RRPA studies of the  $\eta$ -parameter for  $ns \rightarrow \epsilon p$  photoionization in rare gases have been reported.<sup>43</sup> Sizeable polarization is found near the Cooper minima in spite of the non-relativistic

prediction that there should be no spin polarization for the ns photoelectrons.

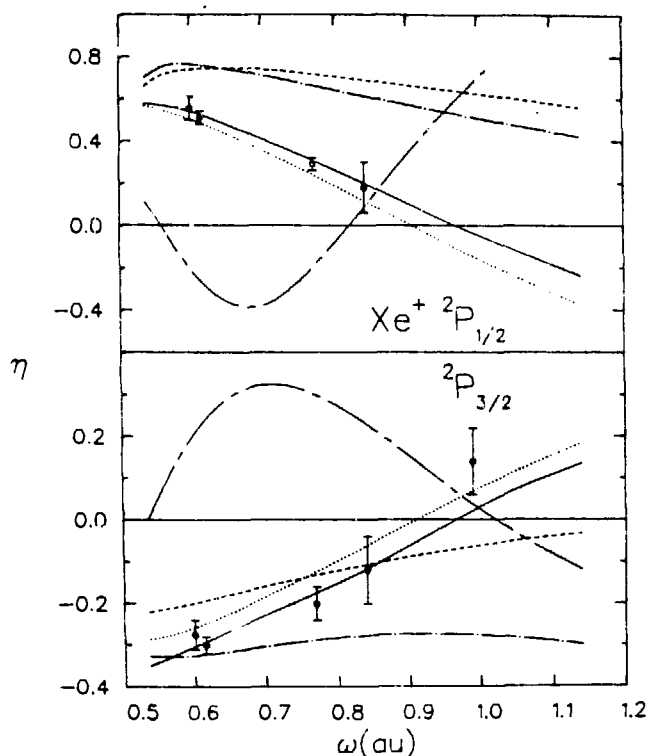


Fig. 7. Spin polarization parameter  $\eta$  of xenon 5p shell photoionization. Experiment: Heinzmann, Schönhense and Kessler, Ref. 72. Theory: ——— RRPA, Ref. 42; ..... Cherepkov, Ref. 73 (note that there is a sign error in this reference); - - - - , ——— , ——— multichannel quantum defect results of Ref. 72 obtained with different sets of parameters from Refs. 74, 75 and 76 respectively.

#### v) Autoionization

To analyze autoionization resonances, it is not convenient to solve the RRPA equations directly, since the computer time required to scan through a family of resonances would be prohibitive. As an alternative, we

use the method of multichannel quantum defect theory (MQDT) pioneered by Seaton<sup>77</sup> and Fano<sup>78</sup> to impose boundary conditions on the RRPA equations. Sets of eigen-channel quantum defect parameters are then obtained at several energies in the autoionizing region of the spectrum. In spite of rapid variations of physical observables such as cross sections, angular distributions, ... etc. in the resonance region, these quantum defect parameters are smooth functions of energy which can be interpolated or extrapolated. At any energy point, we can reconstruct transition amplitudes and hence  $\sigma$ ,  $\beta$ ,  $\eta$ , ... etc. from these parameters. A detailed description of this procedure is given in Ref. 46. Ab initio studies of the inner shell resonances  $1s \rightarrow np$  in Be-like ions<sup>46</sup> and the Beutler-Fano resonances in rare gases<sup>45, 47</sup> have been reported. We shall give an example here to show the validity of this method.

The low lying spectra of the rare gases consists of five interacting Rydberg series, three of which arise from excitations of outer  $p_{3/2}$  electrons to  $ns_{1/2}$ ,  $nd_{3/2}$  and  $nd_{5/2}$  states, and two of which arise from excitations of outer  $p_{1/2}$  electrons to  $ns_{1/2}$  and  $nd_{3/2}$  states (termed  $ns'$  and  $nd'$ , respectively). The first three series converge to the  $2P_{3/2}^0$  threshold, while the remaining two converge to the  $2P_{1/2}^0$  threshold. Between the  $2P_{3/2}^0$  and  $2P_{1/2}^0$  thresholds, we thus have two series of autoionizing resonances - the Beutler-Fano resonances<sup>79, 80</sup> - arising from the  $ns'$  and  $nd'$  states. In Fig. 8, we compare our calculated resonance profiles in xenon with recent experimental measurements by Eland.<sup>81</sup> As one can see, the general features of the autoionization profiles consist of sharp  $ns'$  resonances superimposed on broad  $nd'$  resonances. The observed spectrum is well represented by the theory, except for the rapid decrease in the size of the  $ns'$  peaks which is due to finite instrumental resolution.

In Fig. 9, we compare the RRPA prediction of the angular distribution  $\beta$ -parameters for xenon near the  $(6d', 8s')$  resonances with the measurements of Samson and Gardner,<sup>82</sup> and with two MQDT calculations by Dill<sup>74</sup> and by Geiger<sup>76</sup> based on empirical quantum-defect parameters. The overall agreement is good, except for detailed features near the  $8s'$  resonances.

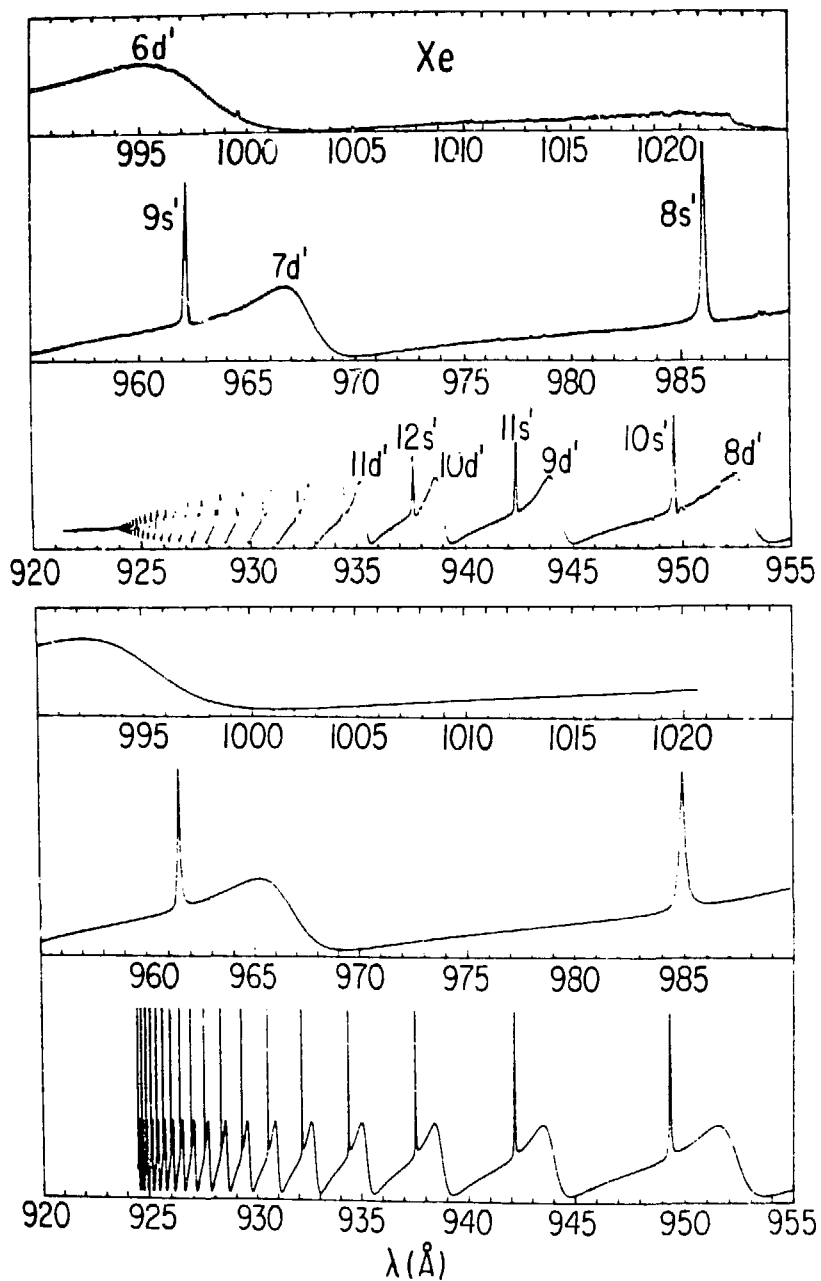


Fig. 8. Photoionization spectra of xenon between the  $2P_{3/2}^o$  and  $2P_{1/2}^o$  thresholds. The upper graph shows experimental data obtained by Eland (Ref. 81) with a photon resolution width of  $0.07 \text{ \AA}$ , and the lower graph shows RRPA results of Ref. 47.

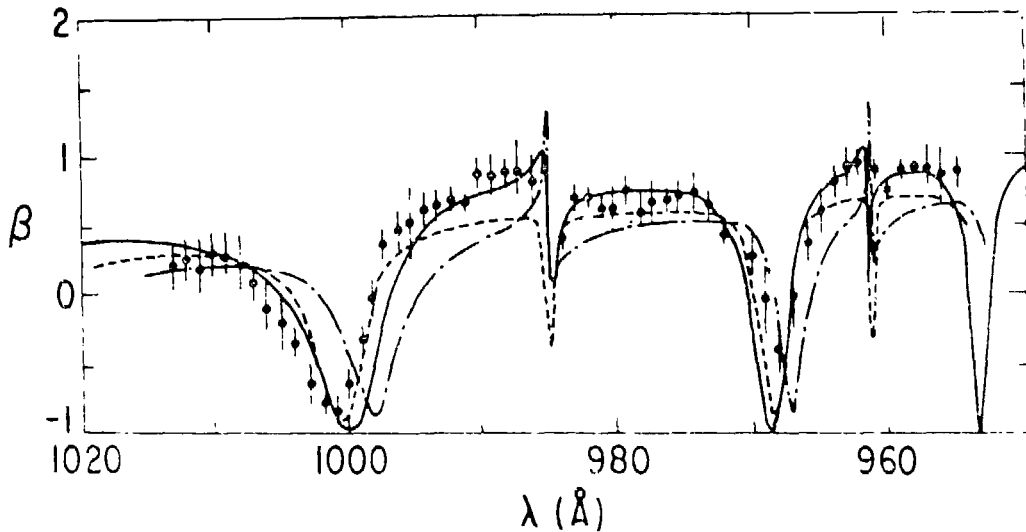


Fig. 9. Angular distribution asymmetry parameters  $\beta$  plotted against photon wavelength  $\lambda$  in the autoionization region of xenon. Experiment:  $\blacklozenge$  Samson and Gardner, Ref. 82. Theory: ——— RRPA, Ref. 47; ——— Dill, Ref. 74; - - - - Geiger, Ref. 76,

### III. CONCLUSION

In the previous sections, we gave a brief review of atomic structure calculations using the RRPA. There are other possible applications of RRPA in addition to those mentioned here. One important application is the study of elastic scattering of photons, together with associated analysis of atomic susceptibilities and shielding factors, especially for high  $Z$  atoms and ions.<sup>33</sup> Another important application of the RRPA is to the study of parity non-conserving (PNC) neutral weak currents in atoms;<sup>34</sup> relativistic RPA studies of core shielding corrections to PNC interaction have been reported by Harris et al.<sup>35</sup>

The RRPA is found to include dominant correction effects in atomic processes and is very successful in dealing with closed shell systems. It is desirable to develop similar relativistic many body techniques for open shell systems.

## ACKNOWLEDGEMENTS

The RRPA is developed through the collaboration of C.D. Lin, A. Dalgarno, P. Shorer, C.M. Lee, K.-N. Huang, V. Radojević and M. LeDourneuf. The work of WRJ is supported in part by the National Science Foundation. The work of KTC is supported by the Division of Basic Energy Sciences of the U.S. Dept. of Energy.

## REFERENCES

1. H.A. Bethe and E.E. Salpeter Quantum Mechanics of One- and Two-Electron Atoms (Spring, Berlin, 1957), p. 170.
2. G.E. Brown and D.G. Ravenhall, Proc. Roy. Soc. (London) A208, 525 (1951).
3. J. Sucher, Phys. Rev. A22, 384 (1980).
4. M.H. Mittleman, Phys. Rev. A5, 2395 (1972).
5. G. Feinberg and J. Sucher, Phys. Rev. Lett. 26, 6811 (1971).
6. M.H. Mittleman, Phys. Rev. A (to be published).
7. I.P. Grant, Adv. Phys. 19, 747 (1970).
8. J.P. Desclaux, Comp. Phys. Comm. 9, 31 (1975).
9. T. Koopmans, Physica 1, 104 (1933).
10. J.A. Bearden and A.F. Burr, Rev. Mod. Phys. 39, 125 (1967).
11. C. Froese Fischer, The Hartree-Fock Method for Atoms (Wiley, New York, 1977).
12. J.R. Mann (private communication).
13. R. Hofstadter, Ann. Rev. Nucl. Sci. 7, 231 (1957).
14. N. Beatham, I.P. Grant, B.J. Kinzie, and S.J. Rose, Physica Scripta 21, 423 (1980).
15. R. Deslattes, Phys. Rev. 186, 1 (1969).
16. J.B. Mann and W.R. Johnson, Phys. Rev. A4, 41 (1971).
17. K.-N. Huang, M. Aoyagi, M.H. Chen, B. Crasemann and H. Mark, Atomic Data and Nuclear Data Tables 18, 243 (1976).
18. A.M. Desiderio and W.R. Johnson, Phys. Rev. A3, 1267 (1971).
19. G.E. Brown, J.S. Langer, and G.W. Schaefer, Proc. Roy. Soc. (London) A251, 92 (1959).
20. P.J. Mohr, Ann. Phys. (N.Y.) 88, 26 (1974); 88, 52 (1974).
21. P.J. Mohr, Phys. Rev. Lett 34, 1050 (1975).
22. K.T. Cheng and W.R. Johnson, Phys. Rev. A14, 1943 (1976).
23. E.H. Wichmann and N.M. Kroll, Phys. Rev. 96, 232 (1954).
24. E.H. Wichmann and N.M. Kroll, Phys. Rev. 101,

- 843 (1956).
25. M. Gyulassy, Phys. Rev. Lett. 33, 921 (1974).
  26. See for example, A.L. Fetter and J.D. Walecka, Quantum Theory of Many-Particle Systems (McGraw-Hill, New York, 1971), p. 156.
  27. W.R. Johnson and C.D. Lin, Phys. Rev. A14, 565 (1976).
  28. M. Ya Amusia and N.A. Cherepkov, Case Studies in Atomic Physics 5, 47 (1975).
  29. C.D. Lin, W.R. Johnson and A. Dalgarno, Phys. Rev. A15, 154 (1977).
  30. W.R. Johnson, C.D. Lin and A. Dalgarno, J. Phys. B9 L303 (1976).
  31. C.D. Lin, W.R. Johnson and A. Dalgarno, Astrophys. J. 217, 1011 (1977).
  32. C.D. Lin and W.R. Johnson, Phys. Rev. A15, 1046 (1977).
  33. P. Shorer, C.D. Lin and W.R. Johnson, Phys. Rev. A16, 1109 (1977).
  34. P. Shorer and A. Dalgarno, Phys. Rev. A16, 1502 (1977).
  35. P. Shorer, Phys. Rev. A18, 1060 (1978).
  36. P. Shorer, Phys. Rev. A20, 642 (1979).
  37. W.R. Johnson and C.D. Lin, J. Phys. B10, L331 (1977).
  38. W.R. Johnson and K.T. Cheng, Phys. Rev. Lett. 40, 1167 (1978).
  39. W.R. Johnson and V. Radojević, J. Phys. B11 L773 (1978).
  40. W.R. Johnson and C.D. Lin, Phys. Rev. A20, 964 (1979).
  41. W.R. Johnson and K.T. Cheng, Phys. Rev. A20, 978 (1979).
  42. K.-N. Huang, W.R. Johnson and K.T. Cheng, Phys. Rev. Lett. 43, 1658 (1979).
  43. K.T. Cheng, K.-N. Huang and W.R. Johnson, J. Phys. B13, L45 (1980).
  44. K.-N. Huang, W.R. Johnson and K.T. Cheng, Phys. Lett. 77A, 234 (1980).
  45. W.R. Johnson and M. LeDourneuf, J. Phys. B13, L13 (1980).
  46. C.M. Lee and W.R. Johnson, Phys. Rev. A22, 979 (1980).
  47. W.R. Johnson, K.T. Cheng, K.-N. Huang and M. LeDourneuf, Phys. Rev. A22, 989 (1980).
  48. A. Dalgarno and G.A. Victor, Proc. R. Soc. A291, 291 (1966).
  49. See, G.F. Brown, Unified Theory of Nuclear Models (North-Holland, Amsterdam, 1967) p. 49,59.
  50. P. Shorer, Thesis, Harvard University (1979).

51. W.R. Johnson, C.D. Lin, K.T. Cheng and C.M. Lee, *Physica Scripta* 21, 409 (1980).
52. K.T. Cheng and W.R. Johnson, *Phys. Rev.* A15, 1326 (1977).
53. K.T. Cheng and W.R. Johnson, *Phys. Rev.* A16, 263 (1977).
54. C.E. Moore, Atomic Energy Levels NSRDS-NBS 35 (U.S. Government Printing Office, Washington, D.C., 1971), Vol. I.
55. R.D. Cowan and K.G. Widing, *Astrophys. J.* 180, 285 (1973).
56. E. Hinnov, *Phys. Rev.* A14, 1533 (1976).
57. J.B. West and J. Morton, *At. Data Nucl. Data Tables* 22, 103 (1978).
58. J.A.R. Samson, *Adv. At. Mol. Phys.* 2, 177 (1966).
59. D.J. Kennedy and S.T. Manson, *Phys. Rev.* A5, 227 (1972).
60. J.A.R. Samson, J.L. Gardner and A.F. Starace, *Phys. Rev.* A12, 1459 (1975).
61. F. Wailleumier, M.Y. Adam, P. Dhez, N. Sandner, V. Schmidt and W. Mehlhorn, *Phys. Rev.* A16, 646 (1977).
62. W. Ong and S.T. Manson, *J. Phys.* B11, L163 (1978).
63. J.L. Dehmer and D. Dill, *Phys. Rev. Lett.* 37, 1049 (1976).
64. M.G. White, S.H. Southworth, P. Kobrin, E.D. Poliakov, R.A. Rosenberg and D.A. Shirley, *Phys. Rev. Lett.* 43, 1661 (1979).
65. N.A. Cherepkov, *Phys. Lett.* 66A, 204 (1978).
66. K.-N. Huang and A.F. Starace, *Phys. Rev.* A21, 697 (1980).
67. W. Ong and S.T. Manson, *J. Phys.* B11, L65 (1978).
68. T.E.H. Walker and J.T. Waber, *J. Phys.* B7, 674 (1974).
69. N.A. Cherepkov, *Sov. Phys.-JETP* 38, 463 (1974).
70. C.M. Lee, *Phys. Rev.* A10, 1598 (1974).
71. K.-N. Huang, *Phys. Rev.* A22, 223 (1980).
72. U. Heinzmann, G. Schönhense and J. Kessler, *Phys. Rev. Lett.* 42, 1603 (1979).
73. N.A. Cherepkov, *J. Phys.* B11, L435 (1978).
74. D. Dill, *Phys. Rev.* A7, 1976 (1973).
75. J. Geiger, *Z. Phys.* A276, 219 (1976).
76. J. Geiger, *Z. Phys.* A282, 129 (1977).
77. M.J. Seaton, *Proc. Phys. Soc.* 88, 801 (1966).
78. U. Fano, *J. Opt. Soc. Am.* 65, 979 (1975).
79. H. Beutler, *Z. Phys.* 93, 177 (1935).
80. U. Fano, *Nuovo Cimento* 12, 154 (1935).
81. See J. Berkowitz, Photoabsorption, Photoionization and Photoelectron Spectroscopy (Academic, New York,

- 1979), p. 181.
82. J.A.R. Samson and J.L. Gardner, Phys. Rev. Lett. 31, 1327 (1973).
83. F.D. Feiock and W.R. Johnson, Phys. Rev. 187, 39 (1969).
84. M.A. Bouchiat and C.C. Bouchiat, Phys. Lett. 48B, 111 (1974); 57B, 284 (1975); J. Physique 35, 899 (1975); 36, 493 (1975).
85. M.J. Harris, C.E. Loving and P.G.H. Sandars, J. Phys. B11, L749 (1978).

#### DISCLAIMER

This report was prepared as an account of work sponsored by an agency of the United States Government. Neither the United States Government nor any agency thereof, nor any of their employees, makes any warranty, express or implied, or assumes any legal liability or responsibility for the accuracy, completeness, or usefulness of any information, apparatus, product, or process disclosed, or represents that its use would not infringe privately owned rights. Reference herein to any specific commercial product, process, or service by trade name, trademark, manufacturer, or otherwise does not necessarily constitute or imply its endorsement, recommendation, or favoring by the United States Government or any agency thereof. The views and opinions of authors expressed herein do not necessarily state or reflect those of the United States Government or any agency thereof.